CHEMISTRY
A EUROPEAN JOURNAL

Design and DNA Binding of an Extended Triple-Stranded Metallo-supramolecular Cylinder

Carsten Uerpmann,[a] Jaroslav Malina,[b] Mirela Pascu,[b] Guy J. Clarkson,[b] Virtudes Moreno,[a] Alison Rodger,[b] Anna Grandas,*[a] and Michael J. Hannon*[b]

Abstract: A new tetracationic triple-stranded supramolecular cylinder is prepared from a bis(pyridylimine) ligand containing a diphenylmethane and two ketimine groups in the spacer. The cylinder is longer and slightly wider than the corresponding cylinder containing just diphenylmethane spacers. Inter-strand CH···π interactions are not observed and this affects the relay of the chiral information within the cylinder; a mixture of *rac* and *meso* isomers results, with the *meso* isomer being the dominant solution species and characterised in the solid state by crystallography. This new cylinder does bind to DNA as confirmed by induced circular dichroism signals in both the metal-to-ligand charge transfer (MLCT) and in-ligand bands of the cylinder. Flow linear dichroism demonstrates that the cylinder binds to DNA in a specific orientation(s) and is consistent with (major) groove-binding as seen for the shorter cylinder. Some DNA bending/coiling is observed but the effect is much less dramatic than observed for the cylinder with diphenylmethane spacers confirming that coiling is not solely a consequence of the tetracationic charge, but rather is related to the precise size and shape of the cylinder.

Keywords: bioinorganic chemistry · DNA recognition · helical structures · noncovalent interactions · supramolecular chemistry

Introduction

For most organisms, DNA encodes the molecular basis of life. Increasing amounts of information about the genetic sequence of ourselves and other species is becoming available, together with enhanced understanding of how this information is processed and regulated and how the processing is influenced by the environment. This offers many potential benefits for the quality of life. In particular, the ability to promote or to prevent the processing of specific genes will be crucial in the fight against many diseases, arising both from under- or over-processing of or damage to our own DNA and arising from external DNAs (as from viruses). For this reason drugs that act on DNA (at specific sequences) and can modulate DNA processing have great potential to form part of the armoury of drugs used within medicine in the 21st century.

Sequence-specific recognition of DNA by biomolecules occurs primarily through non-covalent interactions between the DNA and the surface motifs of proteins, and most commonly (though by no means exclusively) such recognition takes place in the DNA major groove.[1] This groove contains a more diverse pattern of hydrogen bond donor and acceptor units than the minor groove and its size and shape vary more with base sequence. DNA recognition by proteins is also sometimes associated with concomitant bending and coiling.[1] Synthetic agents that recognise DNA, in part because of their smaller size, most usually either intercalate between the base pairs[2] or bind in the minor groove.[3] We have recently demonstrated that metallo-supramolecular assembly may be used to prepare synthetic agents that are a similar size to the DNA recognition motifs found on proteins (such as zinc fingers or α-helices).[4] In particular we have developed metallo-supramolecular cylinders[4,5] that are a similar size and shape to zinc finger units and which do indeed seem to bind in the DNA major groove. Such

[a] Dr. C. Uerpmann, Prof. V. Moreno, Prof. A. Grandas
Departaments de Química Orgànica i Química Inorgànica, Universitat de Barcelona
Martí i Franquès 1–11, 08028 Barcelona (Spain)
Fax (+34) 933-397-878
E-mail: anna.grandas@ub.edu

[b] Dr. J. Malina, M. Pascu, Dr. G. J. Clarkson, Dr. A. Rodger, Dr. M. J. Hannon
Centre for Supramolecular and Macromolecular Chemistry
Department of Chemistry, University of Warwick
Gibbet Hill Road, Coventry, CV4 7 AL (UK)
Fax (+44) 2476-524-112
E-mail: m.j.hannon@warwick.ac.uk

DOI: 10.1002/chem.200401054

metal-based assembly of these cylinders not only allows the nanoscale structure to be created but also imparts cationic charge (the cylinder is a tetracation). This is important since electrostatics will contribute significantly to the strength of the non-covalent binding of such species to the anionic DNA. Fascinatingly, the cylinders not only seem to target the major groove but also induce dramatic intramolecular DNA coiling which is unprecedented with synthetic agents and, in part, reminiscent of DNA coiling induced by histones in the cell nucleus. This is exciting since such coiling might represent a way to prevent gene processing. However, the precise manner in which the molecular-level major groove binding interaction of the cylinder leads to the observed macromolecular DNA coiling effect remains to be elucidated and represents a complex challenge because of the different size-scales on which these two events take place. To try to learn more about the essential design features, we have initiated a programme to investigate the effects of modifications to the basic cylinder structure on both the DNA binding and coiling. Herein we investigate a cylinder system in which we keep the same tetracationic charge as the original cylinder but increase the size of the cylinder unit.

The interaction of metal complexes with DNA has attracted particular interest because cis-platin, and its analogues carboplatin, nedaplatin and oxaliplatin are the most widely used clinical anticancer agents and DNA is believed to be their target.[6] Cis-platin forms metal-nitrogen bonds to N7 of two adjacent purine bases (intra-strand GG and to a lesser extent GA lesions) which causes a kink (~45°) in the DNA which can then be recognised by nuclear HMG proteins. Mononuclear metal complexes that bind through non-covalent interactions (rather than forming bonds from the metal to the nitrogen atoms of the bases) have also been explored: For example, $[Cu(phen)_2]^+$ and "clip-phen" analogues bind in the minor groove and can cause oxidative backbone lesions.[7] $[Ru(phen)_3]^{2+}$ also binds non-covalently to DNA although the precise binding modes of its Δ and Λ enantiomers seems complex.[8] Functionalised analogues in which one phen ligand is extended to form an intercalation site have been developed and these metallo-intercalators may insert either from the major and minor grooves.[9] They have been applied to detect base pair mismatches[10] and rhodium(III) analogues have been used as photoactive footprinting agents.[11] Dinuclear analogues have been prepared which are proposed to thread through the DNA.[12] However none of these various non-covalent DNA-binding metal complexes are reported to exhibit the dramatic intramolecular DNA coiling observed with the cylinder. This may be because they are quite different in size and shape from the cylinders that we have developed, being smaller than the binuclear cylinders and affording smaller molecular surfaces which span only two-to-three DNA base pairs, and as such do not approach the size scale of nature's DNA recognition motifs.

Results and Discussion

To probe the effect of extending the cylinder structure, we made some modifications to the ligand structure. We were keen to try to retain structural similarity with the parent complex, $[Fe_2(L_a)_3]^{4+}$, while simultaneously increasing the dimensions. Our approach was to insert into the ligand design (L_b) ketimine spacer units between the pyridylimine

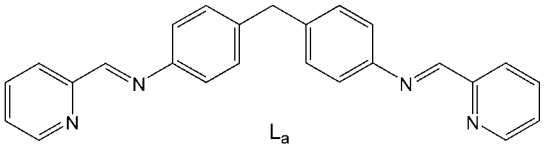

L_a

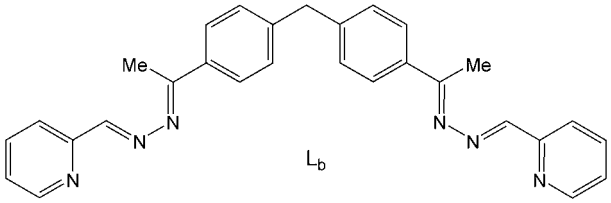

L_b

metal binding units at the ends of the ligand and the diphenylmethane central spacer unit. In this way we aimed to retain the basic structural features found in the original ligand L_a and its complex, but to extend the structure. While we have focused on pyridylimine binding sites in ligands for design of supramolecular architectures, Albrecht et al.[13] and Lehn et al.[14] have explored imine groups as *spacer units* in helicate design; the new design herein combines both approaches.

The ligand L_b was prepared by reaction of 4,4′-diacetyldiphenylmethane with two equivalents of hydrazine and subsequent condensation of the product with pyridine-2-carboxaldehyde to give the ligand. Reaction of the ligand L_b with iron(II) tetrafluoroborate in a chloroform–methanol mix at room temperature afforded the red complex $[Fe_2(L_b)_3][BF_4]_4$. The corresponding chloride salt could be prepared by an analogous route from iron(II) chloride. Electrospray mass spectrometry of an acetonitrile solution of the tetrafluoroborate salt revealed peaks corresponding to $\{Fe_2(L_b)_3(BF_4)_2\}^{2+}$, $\{Fe_2(L_b)_3F\}^{3+}$ and $\{Fe_2(L_b)_3\}^{4+}$ consistent with a dinuclear triple-stranded array.

The IR spectrum shows peaks corresponding to the coordinated ligand and the tetrafluoroborate counterion. The UV/Vis absorption spectrum revealed a band centered at 525 nm ($\varepsilon = 12\,000$) together with a shoulder at 485 nm ($\varepsilon = 10\,000$) corresponding to metal-to-ligand charge transfer (MLCT) transitions which are also observed in other iron(II) polypyridyl[15] and iron(II) pyridylimine complexes[4,5] and which confirm coordination of the iron(II) centre to three pyridylimine units in a low spin configuration. Acetonitrile solutions of the complex retain their red colour, arising from this visible MLCT transition, over a period of days indicating that the complex is stable in acetonitrile solution.

The ^{1}H NMR spectrum of the complex in acetonitrile solution reveals sharp peaks in the region 0–10 ppm confirming the diamagnetic nature of the complex. Two distinct sets of signals are observed in a ratio of about 7:1 indicating the presence of two solution species. Within a dinuclear triple-stranded formulation two configurations are possible: a helical or *rac* isomer in which the stereochemistry of the two metal centres is the same (and the isomer is thus chiral and is one of a pair of enantiomers) and a *meso* isomer in which the stereochemistry is different at the two metal centres rendering the structure achiral.[5,16–18] The central CH_2 resonance of the ligand can be used to distinguish these two isomers.[5,17] In the *rac* isomer the two protons of the CH_2 group are equivalent and give rise to a singlet, whereas in the *meso* isomer they are different and give rise to two doublets and we have previously observed this effect in the dinuclear double-stranded systems of ligand L_a.[17] For this triple-stranded dinuclear complex of L_b we similarly observe a pair of doublets and a singlet for the central CH_2 resonance and this enables us to identify the dominant species (85–90%) as the *meso* isomer and the minor component (10–15%) as the helical *rac* isomers. This contrasts with the iron(II) complex of L_a in which the sole products are the two enantiomeric helical *rac* isomers in both solution and the solid state. This change is presumably a consequence of the greater conformational and tortional flexibility introduced by the additional ketimine units in the spacer and is discussed further below.

Recrystallisation of the tetrafluoroborate salt from an acetonitrile solution by slow diffusion of benzene afforded red crystals which proved suitable for investigation by X-ray diffraction. The crystal structure (Figure 1) reveals a dinuclear

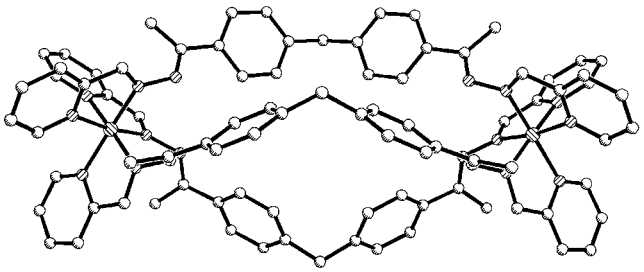

Figure 1. Crystal and molecular structure of the $[Fe_2(L_b)_3]^{4+}$ cation. Hydrogen atoms are omitted for clarity.

triple-stranded cylinder. However, in contrast to the iron(II) complex of the parent ligand L_a which is helical in both solution and the solid state, with ligand L_b the meso isomer crystallises in which the configuration of the two metal centres within the cylinder is opposite leading to an achiral (*meso*) structure. It is pertinent to contrast the structures of the two different cylinders obtained with L_a and L_b (Figure 2 and Figure 3).

As would be anticipated the longer spacer leads to an increase in the metal–metal separation (14.67 Å for the L_b cylinder, 11.52 Å for the L_a cylinder) and an increase of around

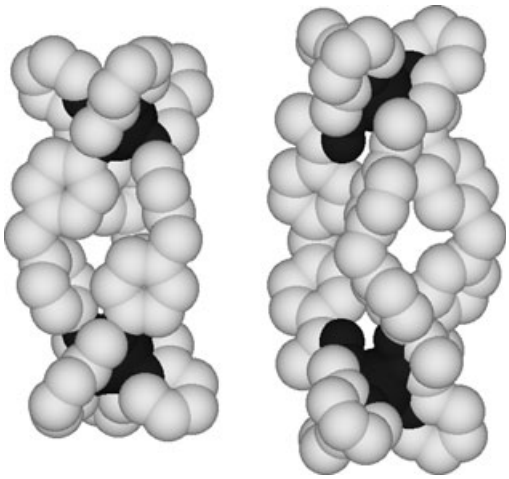

Figure 2. Space-filling representations of the cations *rac*-$[Fe_2(L_a)_3]^{4+}$ (left) and *meso*-$[Fe_2(L_b)_3]^{4+}$ (right). Hydrogen atoms are omitted for clarity.

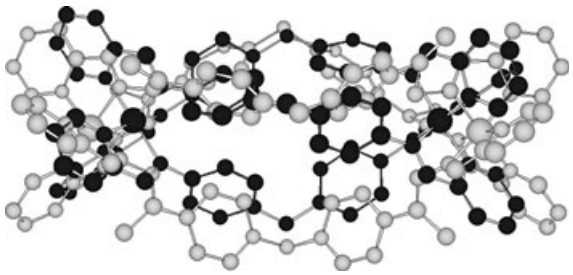

Figure 3. Overlay of the structures of the cations $[Fe_2(L_a)_3]^{4+}$ (dark) and $[Fe_2(L_b)_3]^{4+}$ (light). Hydrogen atoms are omitted for clarity.

12% in the overall length of the cylinder (C···C along the metal–metal vector: 20.38 Å for L_b, 17.34 Å for L_a: H···H 21.92 Å for L_b, 19.46 Å for L_a). The radius of the new L_b cylinder is also increased (measured at the central CH_2 unit 4.66 Å to C; 5.82 Å to H) and is approximately 8% larger than that of the corresponding L_a cylinder (radius 4.43 Å to C; 5.39 Å to H).

While in the complex of L_a the central aryl rings within the cylinder are all face–edge π-stacked together forming CH···π interactions, such interactions are absent in this longer cylinder (Figure 4). The pyridylimine units are planar (pyridylimine torsion angles 0.2°) and the phenyl and ketimine are also approximately coplanar (torsion angles ~23). Twisting within the ligand occurs primarily about the N–N bond between the imine and ketimine units (torsion angles ~85°).

The solid-state and solution structures are also pertinent to a recent report[19] by Albrecht et al. on the 'even-odd principle'[20] in helicate-box formation. In Albrecht's catechol-based systems he notes a tendency for systems with odd numbers of methylene units in the spacer to give *meso* isomers and those with even numbers to give helicates. He attributes this to the energetics associated with the conformation of the methylene chain. In a very recent study aimed at design of "two nanometer-dimensioned" helicates he has

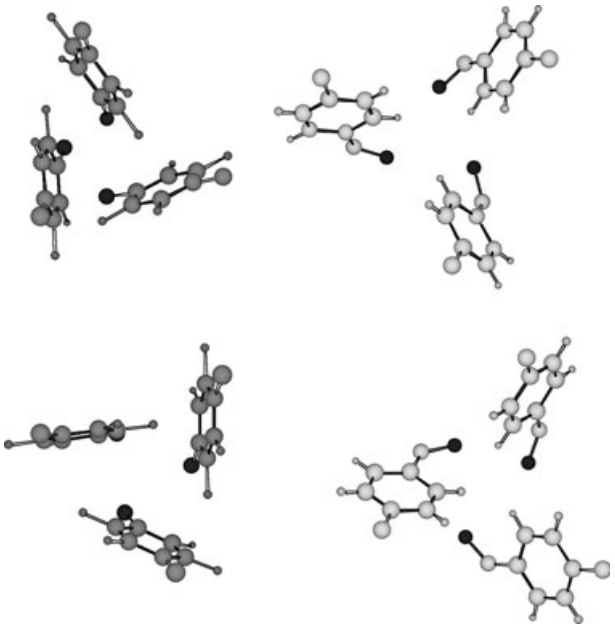

Figure 4. Comparison of the positions of the phenyl rings in the structures of the cations $[Fe_2(L_a)_3]^{4+}$ (left, dark shading) and $[Fe_2(L_b)_3]^{4+}$ (right, light shading) demonstrating the absence of the CH···π interactions in the L_b complex.

employed the diphenylmethane spacer and linked it through imine links to catechol binding units.[19] The result is a ligand in which the chelating units are positioned in a similar fashion to L_b and with titanium(IV) the dicatechol ligand gives a solid-state triple-stranded dinuclear *meso* isomer similar to the pyridylimine structure herein, and only slightly shorter (19.3 Å C···C along the metal-metal vector). To this extent the bis(pyridylimine) *meso* cylinder herein obeys Albrecht's "even-odd principle" as Albrecht's related bis-catechol. The previously reported L_a complex,[5] which is exclusively a triple-helix, is clearly at odds with the "even-odd" principle. Albrecht attributes this to the rigidity of that ligand system which enforces the same chirality at each metal centre.[19] We would concur, noting further that in the L_a system the extensive CH···π interactions at the centre of the complex will further increase the structural rigidity and thus facilitate the relay of the chiral information from one metal centre to the other. In L_b the additional ketimine units provide both additional conformational freedom and move the aryl rings of the spacer apart thereby removing that element of rigidity too. This presumably removes the constraints and allows the spacer conformational energetics associated with the "even-odd principle" to influence the stereochemistry. Nevertheless these constraints may not be completely relaxed as indicated by the presence of 10–15% of the helical *rac* isomer in solution.

DNA binding studies: The tetrafluoroborate salt $[Fe_2(L_b)_3][BF_4]_4$ is soluble in acetonitrile but not water. To investigate whether this salt could be used, the complex was dissolved first in a small amount of acetonitrile and then water was added to give an approximately 20% acetonitrile solution. Within a short time the compound precipitates to give a colourless solution. Consequently DNA binding studies were conducted with the chloride salt $[Fe_2(L_b)_3]Cl_4$. Solutions of the chloride salts, were prepared by dissolving in small amounts of ethanol and then adding water to give a 20% aqueous ethanol solution. We observed a slow change in solution colour from red to orange with time (accompanied by an increase in the MLCT absorption and some changes in the ligand bands). Consequently all solutions used in the spectroscopic investigations were freshly prepared and discarded after one hour.

Circular dichroism (CD) spectroscopy: Titrations of the complex into calf thymus DNA solution were carried out at constant concentrations of DNA (500 μM), NaCl (20 mM) and sodium cacodylate buffer (1 mM). The complex itself shows no CD signal. Any CD signals that arise in the spectroscopic regions of the complex are therefore a consequence of its interaction with the DNA. On addition of the complex to DNA, signals in the MLCT region of the complex (~480 and 520 nm) and in the region of the ligand bands (~315 nm) are observed confirming binding of the cylinder to DNA (Figure 5). These induced signals are simi-

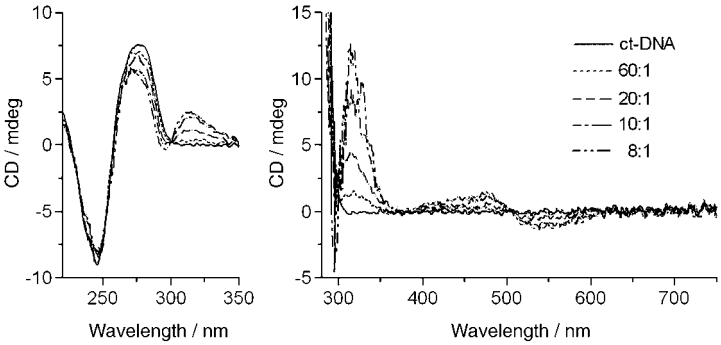

Figure 5. CD spectra of ct DNA (500 μM) in the presence of $[Fe_2(L_b)_3]Cl_4$. Mixing ratio ([DNA]: $[Fe_2(L_b)_3]Cl_4$) is indicated in the figure.

lar to those observed when the L_a triple-stranded cylinder binds to DNA[4] although in this case the sign of the band is inverted. The DNA CD bands (220–300 nm) confirm that the DNA remains in a B-DNA conformation. The increase in CD signal (314 nm) with concentration is linear up to five base pairs: one cylinder consistent with a single binding mode in this regime (from simple size considerations, the cylinder would span five base pairs if groove bound).

Flow linear dichroism (LD) spectroscopy: LD is the difference in absorption of light polarized parallel and perpendicular to an orientation direction. The technique is reliant on orientation of the sample and for DNA we achieve this in solution by orienting the biomacromolecule in a flow Couette cell with orientation through viscous drag.[21] The pri-

mary application of the technique has been to study drug-DNA interactions: if drugs are bound in a specific orientation(s) on the DNA then they too will become orientated, while drugs randomly bound to the DNA or free in solution will not be orientated. Since drugs which are not oriented will have identical absorptions of parallel and perpendicular polarised light, only those drugs which are oriented will exhibit an LD signal. Recently we have recognised that the technique can also be used to probe changes in the orientation of the biomacromolecule induced by drug binding events.[4] Thus for the L_a cylinders we observed dramatic losses of DNA orientation associated with the bending or coiling of the DNA by the cylinder. AFM imaging was able to confirm that this arose from an intramolecular DNA coiling effect.

To probe the binding of $[Fe_2(L_b)_3]Cl_4$, titrations were carried out at constant concentrations of DNA (500 μM), NaCl (20 mM) and sodium cacodylate buffer (1 mM). The presence of bands corresponding to cylinder transitions (~315, 520 nm) in the LD spectrum (Figure 6) confirms that the

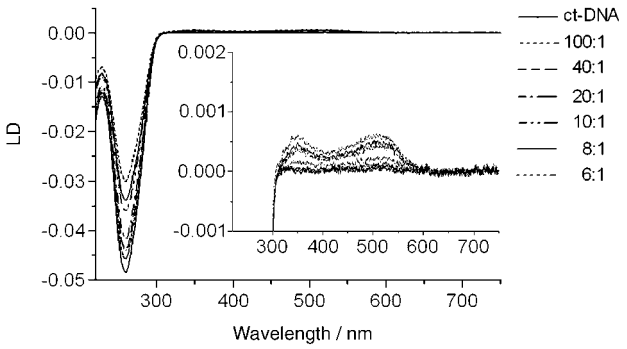

Figure 6. LD spectra of ct DNA (500 μM) in the presence of $[Fe_2(L_b)_3]Cl_4$. Mixing ratio ([DNA]: $[Fe_2(L_b)_3]Cl_4$) is indicated in the figure.

cylinder binds to DNA and does so in specific orientation(s). Some DNA bending or coiling is also observed as evidenced by the decrease in the DNA band at 260 nm. The loss of orientation is not as dramatic as that observed with the L_a iron(II) cylinder: In the LD of the DNA region the parent *P* enantiomer of the L_a cylinder causes a 75% loss of orientation at a 15:1 ratio and the *M* enantiomer is even more aggressive in its coiling causing a 95% loss at a 20:1 ratio. This new L_b cylinder shows a loss of only about 40% at 6:1.

Thermal stability: Thermal stability experiments (monitored by measuring cylinder absorbance at 476 nm) indicated that the complex was degraded as the temperature was increased above ambient and that the presence of DNA had no significant stabilising effect on the complex. For this reason, it is unsurprising that the cylinder also exhibited no effect on the melting temperature of ct-DNA.

Conclusion

The additional ketimine groups introduced into the spacer unit of L_b increase the separation of the two metal binding sites in the ligand and, as expected, extend the length of the cylinder created. However they also move the phenylene groups on different ligand strands apart and these phenylenes no longer form the inter-strand CH···π interactions observed in the complex of L_a. This affects the complex in several ways. The removal of the inter-strand interactions makes the relay of the chiral information from one metal centre to the other less effective and a mixture of *rac* and *meso* isomers results, with the *meso* isomer being dominant. We have recently demonstrated that inter-strand interactions are important in obtaining exclusively *rac* isomers in the related *double*-stranded systems.[17a] The diameter of the cylinder is also increased with respect to the L_a cylinder. The stability of the complex in aqueous solution is reduced, supporting the view that the inter-strand CH···π interactions do contribute to the stability of the complexes of ligand L_a.

This new cylinder does bind to DNA as evidenced by the observation of induced CD signals in the both the MLCT and in-ligand bands of the cylinder. The induced signals are similar to those observed for the L_a complex although opposite in sign. We speculate that this may be related to the fact that the L_a cylinder is *rac*, whereas the L_b cylinder is predominantly the *meso* isomer and contains metal centres with opposite configurations which will have diferent transition orientations. The lower aqueous stability of the L_b cylinder makes it difficult to explore this further. The flow LD experiment confirms that the L_b cylinder binds to DNA in a specific orientation(s) (as the L_a cylinder). The sign of the cylinder MLCT LD signal precludes this being an intercalative binding mode (consistent with the cylinder's large size and shape) but is consistent with a (major) groove-binding mode as seen for the L_a cylinder.

Some DNA bending/coiling is observed but the effect is much less dramatic than observed for the L_a cylinder. It is clear from this result that the DNA coiling observed with the L_a cylinder is not solely a consequence of the tetracationic charge, but rather is related to the precise size and shape of the cylinder. We are currently investigating other related cylinder designs to try to probe further the essential features of the design and their impact on the DNA recognition and coiling.

Experimental Section

General: All reagents and solvents were purchased from commercial sources (Aldrich, Fluorochem, Acros, Fluka) and used without further purification. NMR spectra were recorded on Varian Gemini 2000 (200 MHz) or Brüker DPX 400 (400 MHz) instruments at 298 K using standard Varian or Brüker software. FAB mass spectra were recorded on a Micromass VG-Quattro System or a Micromass AutoSpec spectrometer using 3-nitrobenzyl alcohol as matrix. ESI mass spectra of the complex were recorded on a Micromass Quatro II (low-resolution triple quadrupole mass spectrometer) instrument at the EPSRC National Mass Spec-

trometry Centre, University of Wales, Swansea and of the ligand on an Micromass ZQ System at U. Barcelona. Infrared spectra (solid pellets or films prepared by evaporation of solutions mounted on NaCl plates) were measured with a Perkin Elmer Paragon 1000 FTIR spectrometer or a Nicolet 510 FT-IR Spectrometer. UV/Vis measurements were made using a Jasco V-550 spectrophotometer.

Ligand L_b: 4,4′-Diacetyldiphenylmethane (0.508 g, 2 mmol) was dissolved in methanol (15 mL). Hydrazine monohydrate (0.210 g, 4.2 mmol) was added slowly over a period of 15 minutes and the mixture was stirred at room temperature overnight. The white precipitate of the bishydrazone formed (0.450 g, 1.6 mmol, yield 80%) was collected by filtration, washed with small portions of cold methanol (2×5 mL) and dried in vacuo.

^{1}H NMR (200 MHz, $CDCl_3$): $\delta = 7.56$ (d, $J = 8.2$ Hz, 4H; Ph), 7.16 (d, $J = 8.2$ Hz, 4H; Ph), 5.32 (s, 4H; NH_2), 3.98 (s, 2H; CH_2), 2.11 ppm (s, 6H; CH_3); ^{13}C NMR (50 MHz, $CDCl_3$): δ 11.7, 41.3, 125.5, 128.8, 140.8, 147.3 ppm; MS (+ve FAB, NBA): *m/z*: 281 $[M+H]^+$; IR (film): $\tilde{\nu} =$ 3354 s, 3220 s, 3083 m, 1654 m, 1604 m, 1509 m, 1436 m, 1368 m, 1335 m, 1108 m cm^{-1}.

The bis(hydrazone) (0.135 g, 0.48 mmol) and pyridine-2-carboxaldehyde (0.107 g, 1 mmol) were mixed in methanol (15 mL). After adding several drops of acetic acid the clear solution was stirred at room temperature overnight. The resulting yellow precipitate was collected by filtration and dried in vacuo (0.202 g, 0.44 mmol, yield 91%).

$R_f = 0.31$ (silica; CH_2Cl_2:MeOH 98:2); ^{1}H NMR (200 MHz, $CDCl_3$): $\delta =$ 8.68 (d, $J = 4.4$ Hz, 2H; py-H6), 8.41 (s, 2H; N=CH), 8.14 (d, $J = 7.8$, , 2H; py-H3), 7.86 (d, $J = 8.4$ Hz, 4H; Ph), 7.73 (td, $J = 7.5$, 1.8 Hz, 2H; py-H4), 7.35 (ddd, $J = 7.2$, 4.8, 1.1 Hz, 2H; py-H5), 7.25 (d, $J = 8.2$ Hz, 4H; Ph), 4.08 (s, 2H; CH_2), 2.47 ppm (s, 6H; CH_3); ^{13}C NMR (50 MHz, $CDCl_3$): δ: 15.4, 41.6, 121.5, 124.5, 127.2, 129.0, 136.4, 143.0, 149.6, 153.6, 157.1, 163.9 ppm; IR (film): $\tilde{\nu} =$ 3095 m, 1649 m, 1610 s, 1436 m, 1369 m, 1343 m, 1115 m cm^{-1}; MS (+ve FAB, NBA): *m/z*: 459 $[M+H]^+$; MS (+ve ESI): *m/z*: 459 $[M+H]^+$; elemental analysis calcd(%) for $C_{29}H_{26}N_6$: C 76.0, H 5.7, N 18.3; found: C 76.0, H 5.7, N 18.1.

Iron(II) complex: L_b (0.023 g, 0.05 mmol) and iron(II) tetrafluoroborate (0.025 g, 0.075 mmol) in a mixture chloroform–methanol (1:1) were stirred for 6 h at room temperature. The red precipitate was collected by vacuum filtration, washed with methanol and dried in vacuo under P_4O_{10} (0.021 g, 70%). X-ray quality, red crystals were obtained by slow diffusion of benzene into a solution of the complex in acetonitrile. The chloride salt was prepared by an analogous route from iron(II) chloride.

^{1}H NMR (400 MHz, CD_3CN, 298 K): $\delta = 8.31$ (s, 2H; H^{imine} *helix*), 8.25 (s, 14H; H^{imine} *box*), 8.18 (m, 16H; H^4), 8.09 (m, 16H; H^3), 7.79 (d, $J =$ 8.3 Hz, 28H; Ph *box*), 7.66 (d, $J = 8.0$ Hz, 4H; Ph *helix*), 7.59 (m, 32H; H^5& H^6), 7.33 (d, $J = 8.3$ Hz, 28H; Ph *box*), 7.20 (d, $J = 8.0$ Hz, 4H; Ph *helix*), 4.09 (s, 2H; CH_2 *helix*), 4.06 (d, $J = 23$ Hz, 7H; CH_2 *box*), 3.96 (d, $J = 23$ Hz, 7H; CH_2 *box*), 1.27 (s, 6H; CH_3 *helix*), 1.20 (s, 42H; CH_3 *box*); ^{1}H NMR (400 MHz, CD_3OD, 298 K, chloride salt): $\delta = 8.58$ (s, 2H; H^{imine} *helix*), 8.532 (s, 14H; H^{imine} *box*), 8.30 (m, 16H; H^4), 8.24 (m, 16H; H^3), 7.98 (d, $J = 8.0$ Hz, 28H; Ph *box*), 7.84 (d, $J = 7.8$ Hz, 4H; Ph *helix*), 7.75 (m, 32H; H^5& H^6), 7.37 (d, $J = 8.0$ Hz, 28H; Ph *box*), 7.20 (d, $J =$ 8.0 Hz, 4H; Ph *helix*), 4.13 (s, 2H; CH_2 *helix*), 3.97 (d, $J = 14$ Hz, 7H; CH_2 *box*), 3.88 (d, $J = 14$ Hz, 7H; CH_2 *box*), 1.34 (s, 48H; CH_3 *helix* & CH_3 *box*); IR (solid): $\tilde{\nu} =$ 1600 m, 1562w,1472 m, 1439w, 1413w, 1371w, 1306 m, 1187w, 1162w, 1053 s, 919w, 813w, 777 s, 760 s, 686w cm^{-1}; UV/Vis (MeCN): $\lambda = 525$ ($\varepsilon = 12000$), 485 nm ($\varepsilon = 10000$), 296 nm ($\varepsilon =$ 138000), 260 nm ($\varepsilon = 95000$); MS (+ve ESI, MeCN): *m/z*: 372 $\{Fe_2(L_2)_3\}^{4+}$ (100%), 502 $\{Fe_2(L_2)_3F\}^{3+}$ (10%), 830 $\{Fe_2(L_2)_3(BF_4)_2\}^{2+}$ (5%).

X-ray crystallography: Crystal structure data for $C_{43.8}H_{42.8}B_{1.33}F_{5.33}Fe_{0.67}N_{7.4}O_{0.5}$, $M_r = 833.83$, hexagonal, space group *P*6(3)/*m*, $a = 13.791(3)$, $b =$ 13.791(3), $c = 44.622(10)$ Å, $U = 7349(3)$ Å^3, $Z = 6$, $\rho_{calcd} = 1.130$ g cm^{-3}, $\mu(Mo_{K\alpha}) = 0.270$ mm^{-1}. Character: purple blocks $0.28 \times 0.28 \times 0.04$ mm. A total of 30463 reflections were measured, 3620 unique[R(int) = 0.1462]. Goodness-of-fit on F^2 was 1.051. $R1$ [for 2373 reflections with $I > 2\sigma(I)$] = 0.0883, $wR2 = 0.2225$. Data/restraints/parameters 3620/22/327. Crystal data was collected at 180(2) K with a Siemens-SMART-CCD diffractometer[22] equipped with an Oxford Cryosystem Cryostream Cooler.[23] Refinements used SHELXTL.[24] Systematic absences indicated space group *P*6(3)/*m* or *P*6(3). The former was chosen on the basis of intensity statistics and shown to be correct by successful refinement. The structure was solved by direct methods with additional light atoms found by Fourier methods. Hydrogen atoms were added at calculated positions and refined by using a riding model with freely rotating methyl groups. Anisotropic displacement parameters were used for all non hydrogem atoms; hydrogen atoms were given isotropic displacement parameters equal to 1.2 (or 1.5 for methyl hydrogen atoms) times the equivalent isotropic displacement parameter of the atom to which the hydrogen atom is attached.

The asymmetric unit contains half a ligand, an iron, a benzene molecule, two partially occupied acetonitriles (N200–C202, 50% occupancy and N400–C402, 20% occupancy) two partially occupied water molecules and two very disordered BF_4 counter ions (as detailed below). Fe1 sits on special position 4f on a three-fold axis. C18, the central methylene of the ligand lies on a mirror plane, special position 6h. B10 sits on special position 4f on a three-fold axis and has the fluorine atoms disordered over two positions in a 3:1 ratio. The major position F11/F12 has F11 on the same three-fold axis and F12 in a general position. The minor component F11 A/F12 A has F11 A on the three-fold axis and F12 A in a general position. B20 sits on special position 4e on a three fold axis and has very disordered fluorine atoms over at least three positions. This was modelled by placing four fluorine atoms (F21–F24) on B20 and making the sum of their occupancies add up to a BF_4. Acetonitrile N400–C402, as well as being only partially occupied lies on the mirror plane, special position 6h. Some additional electron density was modelled as partially occupied water molecules O600 and O700. O600 lies on special position 4f on a three-fold axis and is 50% occupied. O700 lies on special position 4e on a three-fold axis and is 25% occupied. The partial solvent occupancies and no hydrogen atoms on the water molecules explains the fractional formula.

CCDC-252893 contains the supplementary crystallographic data for this paper. These data can be obtained free of charge from The Cambridge Crystallographic Data Centre via www.ccdc.cam.ac.uk/data_request/cif.

Biophysical experiments: *Circular dichroism*: Spectra were collected in 1 cm pathlength cuvettes (280–850 nm) or 2 mm pathlength cuvettes (220–350 nm) using a Jasco J-715 spectropolarimeter. Spectroscopic titrations were performed in which CD and UV/Vis absorbance spectra were collected. Titrations were carried out at constant concentrations of DNA (500 μM), NaCl (20 mM) and sodium cacodylate buffer (1 mM). The DNA:metal complex ratio was decreased during the titration series by incrementing the concentration of metal complex in the cuvette from 0–62.5 μM. Titrations were performed so as the concentrations of DNA, NaCl and sodium cacodylate buffer in the cuvette remained unaltered.[25]

Flow linear dichroism: Flow *LD* spectra were collected by using a flow couette cell in a Jasco J-715 spectropolarimeter adapted for LD measurements. Long molecules, such as DNA (minimum length of ~250 base pairs), can be orientated in a flow couette cell. The flow cell consists of a fixed outer cylinder and a rotating solid quartz inner cylinder separated by a 0.5 mm wide gap giving a total 1 mm pathlength.[21]

Thermal stability measurements: Thermal stability experiments used a thermostatic cell-changer UV/Vis spectrophotometer on a Cary1E spectrophotometer in masked 1.2 mL cuvettes, monitoring cylinder absorbance at 476 nm.

Acknowledgements

We thank the European Union (MARCY RTN, HPRN-CT-2002–00175; Marie Curie fellowships: M.P. HPMT-GH-01–00365–11; J. M. HPMF-CT-2002–01856); the Spanish MEC (BQU2001–3693-C02–01) and the Generalite de Catalunya (2001SGR49 and Centre de Referencia de Biotechnologia) for funding. This work was conducted in the context of COST D20 WG D20/0010/02 on non-covalent DNA recognition. We thank EPSRC and Siemens Analytical Instruments for grants in support of the diffractometer and the EPSRC National Mass Spectrometry Service Centre,

Swansea for recording electrospray mass spectra. M.J.H. is the Royal Society of Chemistry Sir Edward Frankland Fellow 2004–2005.

[1] See for example: J. M. Berg, J. L. Tymoczko, L. Stryer, *Biochemistry*, 5th ed., Freeman, New York, **2002**; C. Branden, J. Tooze, *Introduction to Protein Structure*, 2nd ed., Garland, New York, **1999**; S. Neidle *Nucleic Acid Structure and Function*, OUP, Oxford, **2002**; R. E. Dickerson, *Nucleic Acids Res.* **1998**, *26*, 1906–1926.

[2] See for example: B. C. Baguley, *Anti-Cancer Drug Des.* **1991**, *6*, 1–35; S. J. Lippard, J. M. Berg, *Principles of Bioinorganic Chemistry* University Science Books, Mill Valley, CA, **1994**; P. B. Glover, P. R. Ashton, L. J. Childs, A. Rodger, M. Kercher, R. M. Williams, L. De Cola, Z. Pikramenou, *J. Am. Chem. Soc.* **2003**, *125*, 9918–9919.

[3] P. B. Dervan, B. S. Edelson, *Curr. Biol. Curr. Opin. Struc. Biol.* **2003**, *13*, 284–299; P. B. Dervan, *Bioorg. Med. Chem.* **2001**, *9*, 2215–2235.

[4] a) M. J. Hannon, V. Moreno, M. J. Prieto, E. Moldrheim, E. Sletten, I. Meistermann, C. J. Isaac, K. J. Sanders, A. Rodger, *Angew. Chem.* **2001**, *113*, 903–908; *Angew. Chem. Int. Ed.* **2001**, *40*, 880–884; b) I. Meistermann, V. Moreno, M. J. Prieto, E. Moldrheim, E. Sletten, S. Khalid, M. Rodger, J. Peberdy, C. J. Isaac, A. Rodger, M. J. Hannon, *Proc. Natl. Acad. Sci. USA* **2002**, *99*, 5069–5074; c) E. Moldrheim, M. J. Hannon, I. Meistermann, A. Rodger, E. Sletten, *J. Biol. Inorg. Chem.* **2002**, *7*, 770–780; d) M. J. Hannon, A. Rodger, *Pharmaceutical Visions* **2002**, autumn issue, 14.

[5] M. J. Hannon, C. L. Painting, J. Hamblin, A. Jackson, W. Errington, *Chem. Commun.* **1997**, 1807–1808.

[6] *Cisplatin, Chemistry and Biochemistry of a Leading Anti-Cancer Drug* (Ed.: B. Lippert) Wiley-VCH, Weinheim, Germany, **1999**; J. Reedijk, *Chem. Commun.* **1996**, 801–806; Z. J. Guo, P. J. Sadler, *Adv. Inorg. Chem.* **2000**, *49*, 183–306 and references therein.

[7] D. S. Sigman, T. W. Bruice, A. Mazumder, C. L. Sutton, *Acc. Chem. Res.* **1993**, *26*, 98–104; M. Pitié, B. Donnadieu, B. Meunier, *Inorg. Chem.* **1998**, *37*, 3486–3489.

[8] C. V. Kumar, J. K. Barton, N. J. Turro, *J. Am. Chem. Soc.* **1985**, *107*, 5518–5523; C. Hiort, B. Nordén, A. Rodger, *J. Am. Chem. Soc.* **1990**, *112*, 1971–1982; D. Z. Coggan, I. S. Haworth, P. J. Bates, A. Robinson, A. Rodger, *Inorg. Chem.* **1999**, *38*, 4486–4497.

[9] K. E. Erkkila, D. T. Odom, J. K. Barton, *Chem. Rev.* **1999**, *99*, 2777–2795; I. Greguric, J. R. Aldrich-Wright, J. G. Collins, *J. Am. Chem. Soc.* **1997**, *119*, 3621–3622; E. Tuite, P. Lincoln, B. Norden, *J. Am. Chem. Soc.* **1997**, *119*, 239–240; P. Lincoln, E. Tuite, B. Norden, *J. Am. Chem. Soc.* **1997**, *119*, 1454–1455.

[10] K. E. Erkkila, B. P. Hudson, J. K. Barton, D. C. Rees, *Nat. Struct. Biol.* **2000**, *7*, 117–121; U. Schatzschneider, J. K. Barton, *J. Am. Chem. Soc.* **2004**, *126*, 8630–8631; E. Ruba, J. R. Hart, J. K. Barton, *Inorg. Chem.* **2004**, *43*, 4570–4578.

[11] H. Junicke, J. R. Hart, J. Kisko, O. Glebov, I. R. Kirsch, J. K. Barton, *Proc. Natl. Acad. Sci. USA* **2003**, *100*, 3737–3742; B. A. Jackson, J. K. Barton, *J. Am. Chem. Soc.* **1997**, *119*, 12986–12987.

[12] B. Önfelt, P. Lincoln, B. Nordén, *J. Am. Chem. Soc.* **2001**, *123*, 3630–3637.

[13] See for example M. Albrecht, I. Janser, S. Kamptmann, P. Weis, B. Wibbeling, R. Fröhlich, *Dalton Trans.* **2004**, 37–43.

[14] K. M. Gardinier, R. G. Khoury, J. M. Lehn, *Chem. Eur. J.* **2000**, *6*, 4124–4131; R. Stiller, J. M. Lehn, *Eur. J. Inorg. Chem.* **1998**, 977–982.

[15] E. C. Constable, *Adv. Inorg. Chem. Radiochem.* **1986**, *28*, 69–121; E. C. Constable, *Adv. Inorg. Chem.* **1989**, *34*, 1–63.

[16] L. J. Childs, M. J. Hannon, *Supramol. Chem.* **2004**, *16*, 7–22; M. Albrecht, *Chem. Rev.* **2001**, *101*, 3457–3497; C. Piguet, G. Bernardinelli, G. Hopfgartner, *Chem. Rev.* **1997**, *97*, 2005–2062.

[17] a) L. J. Childs, M. Pascu, A. J. Clarke, N. W. Alcock, M. J. Hannon, *Chem. Eur. J.* **2004**, *10*, 4291–4300; b) M. J. Hannon, C. L. Painting, N. W. Alcock, *Chem. Commun.* **1999**, 2023–2024; c) L. J. Childs, M. J. Hannon, N. W. Alcock, *Angew. Chem.* **2002**, *114*, 4418–4420; *Angew. Chem. Int. Ed.* **2002**, *41*, 4244–4247.

[18] A. Bilyk, M. M. Harding, P. Turner, T. W. Hambley, *J. Chem. Soc. Dalton Trans.* **1994**, 2783–2790; C. O. Dietrich-Buchecker, J. F. Nierengarten, J. P. Sauvage, N. Armaroli, V. Balzani, L. DeCola, *J. Am. Chem. Soc.* **1993**, *115*, 11237–11244.

[19] M. Albrecht, I. Janser, H. Houjou, R. Fröhlich, *Chem. Eur. J.* **2004**, *10*, 2839–2850.

[20] M. Albrecht, *Chem. Eur. J.* **2000**, *6*, 3485–3489.

[21] A. Rodger, B. Norden, *Circular and Linear Dichroism*, Oxford University Press, Oxford, **1997**.

[22] SMART user's manual, Siemens Industrial Automation Inc., Madison, WI, **1994**.

[23] J. Cosier, A. M. Glazer, *J. Appl. Crystallogr.* **1986**, *19*, 105–107.

[24] G. M. Sheldrick, *Acta Crystallogr. Sect. A* **1990**, *46*, 467–473.

[25] A. Rodger, *Methods Enzymol.* **1993**, *226*, 232–258.

Received: October 15, 2004
Published online: January 25, 2005